'Fragile Bits' vs. Multi-Enrollment - A Case Study of Iris Recognition on Bath University Iris Database

Nicolaie Popescu-Bodorin, *Member, IEEE*
Department of Mathematics and Computer Science,
Spiru Haret University, Bucharest, Romania
http://fmi.spiruharet.ro/bodorin/

Abstract

This paper explores the use of *fragile bits* in the context of a recently proposed iris recognition methodology based on Circular Fuzzy Iris Segmentation and Gabor Analytic Iris Texture Binary Encoder. Iris images from Bath University Iris Database are encoded as iris codes at three different lengths (192, 512, 768 Bytes) and used to test the concept of *fragile bits*. Six iris recognition tests are presented in order to illustrate the efficiency of the recently proposed iris recognition methodology in both single-enrollment and multi-enrollment iris recognition scenarios. Three additional tests show that at least in the recognition scenarios presented here, using a certain type of *fragile bits* will determine a split of the set of genuine scores into two distributions having two completely different statistics, case in which apparent improvements of the recognition performance measured through decidability index and through Fisher's ratio are irrelevant. Also, some important differences between different types of *fragile bits* are stated here for the first time.

Key words: iris recognition, iris segmentation, circular fuzzy iris segmentation, Gabor analytic iris texture binary encoder, fragile bits;
2000 AMS subject classifications: 68T10, 68U10, 68N99, 44A15.

1 Introduction

From the early stages of our PhD study we found that an open problem in iris recognition is the fact that we can't say for sure if a given iris database is or isn't a representative sample. To be more precise, if the length of the iris binary code is assumed to be 1024, then the numerical space representing the iris population counts more than $1.7E{+}308$ elements. Now, let's imagine a huge iris database containing, let's say, $1E+12$ images and assume that extraordinary iris recognition results have been proved using this database. We should use some sampling techniques enabling us to extrapolate these

results to entire iris code population (and to other similar databases, in particular), despite the fact that representativity rate of our hypothetical database is nearly null ($1E-296$). Unfortunately, such techniques don't exist and consequently, in these circumstances, explaining the differences between theoretical and experimental results could prove to be difficult and misleading. A possible example is the concept of *fragile bits*, initially introduced to explain the difference between experimentally determined False Reject Rates and the theoretically predicted values.

As an alternative, we consider that the set of all available iris-codes is so sparse and scattered within the iris-code population that the matching between the bits of any two different irides happens only by chance. This is the first major hypothesis in our approach to iris recognition. It was initially formulated by Daugman in the early 90s but never fully exploited ever since. Present paper shows that accepting and following this hypothesis leads to theoretical and experimental iris recognition results agreeing each other. In this scenario we will give here some examples showing that masking the so called *fragile bits* don't necessary improve the iris recognition performance.

The concept of *fragile bits* was proposed by Bolle and all [1] but the first work truly investigating this subject is very recent indeed (Hollingsworth and all [4]). The cited paper introduces *fragile bits* in two ways: first, as a mask of unstable bits that are flipping from 0 to 1 or vice versa in a chosen number of observations, and second, as a mask of the bits that are more susceptible to flip because of a phase instability phenomenon: in one particular observation, a bit is considered to be *fragile* if the corresponding complex value encoding the corresponding iris pixel is located close to the real or imaginary axis. But, in fact, the two cases describe two different concepts:

- In the first case, *fragile bits* are defined as an *a priori knowledge* inferred from a given number of previous observation as a mask containing the pixels that are proven to be unstable by their values, but the causality of this instability is not evident. In this context, it is very important to answer the following questions: is this mask a feature of the iris or it is just a feature of the given set of observations? Does it depend on the iris texture or on the variability of the acquisition conditions?
- As defined in the second case, the concept of *fragile bits* represents, in fact, an *a posteriori knowledge* about the current observation(s), a mask defined by a fuzzy membership assignment conditioned by the degree of closeness to the real/imaginary axis or, as mentioned in [4], by an adaptive thresholding of the lowest quartile calculated for the histogram of the set containing the absolute values corresponding to the complex representation of the unwrapped iris.
- To test the concept of *fragile bits* in the first scenario, the current iris codes will be compared to the stored template gallery using the mask of *fragile bits* computed for the enrolled identities. The results of the tests could give

the answers to the questions formulated above. But, the most important outcome of such a test will be to find out if the use of *fragile bits* is or isn't compatible with the hypothesis that the matching between the bits of any two different irides happens only by chance.
- In the second scenario, testing the concept of *fragile bits* means to assume that any two iris codes will be compared using a mask computed at run-time. The best possible outcome of such a test would be an improvement in the system performance quantified as a narrowing of the genuine or /and imposter score distributions, an increase of the distance between the two classes of scores, or an improvement of other values calculated as evaluation criteria (decidability index, Fisher's ratio, [17])

We must clarify that we call *a priori knowledge* any piece of knowledge/data used to bring the biometric system in a fully functional ready state able to treat the client recognition request. One notable difference between the above two cases is that in the former, *a priori knowledge* includes the (stored) masks of *fragile bits* for all enrolled identities, while in the latter, *a priori knowledge* includes a method to produce (at run-time) a mask for any given pair of iris codes. From the beginning, it can be remarked that if the mask of *fragile bits* mainly depends on other things than the iris texture, at least one from the above tests will fail to improve recognition performance.

2 Circular Fuzzy Iris Segmentation

The segmentation algorithm presented here was proposed in [12] as an alternative to the currently available segmentation procedures that use integro-differential Daugman operator [2], or Hough Transform [16], or active contours [3]. The most important difference between previous segmentation methods and CFIS is the dimension of the parameter space needed to be searched in order to find pupillary and limbic boundary: in CFIS procedure iris boundaries are found by solving one dimensional optimization problems.

CFIS procedure consists in the following operations: pupil finding and limbic boundary circular approximation. Pupillary and limbic boundaries are assumed to be concentric circles.

An anatomic argument for using this hypothesis is that since the pupil is nearly circular, there must be a circular concentric iris ring controlling the pupil movements. Such a circular iris ring is expected to play the most important role in iris recognition, despite the fact that it appears to be a rough approximation of the actual iris.

A system requirement sustaining the above formulated hypothesis is that the segmentation routine must be fast and energy-efficient. Nearly lossless unwrapping of the iris can be computed using a polar / bipolar coordinate transform depending on the type assumed for the iris: concentric / eccen-

tric circular ring. The latter is computationally more expensive than the former because the eccentricity varies from a sample to another and consequently, one bipolar mapping must be (re)computed for each sample (eye image). When the iris ring is assumed to be concentric, the polar mapping is computed once for all samples, during program initialization.

2.1 Fast Pupil Finder Algorithm

The proposed pupil finder algorithm can be stated as follows:

```
Fast Pupil Finder Algorithm (N. Popescu-Bodorin):
INPUT: the eye image IM;
1.Extract the pupil cluster (Fig.1.a):
   PC = fkmq(IM,16);
   PC = (PC == min(PC(:)));
2.Compute horizontal and vertical Run Length
  quantization of PC (Fig.2.a-b):
   RLV(:,,j) = vrleq(PC);
   RLH(j,:) = hrleq(PC);
3.Compute the pupil indicator PI (Fig.2.c):
   [k, PI] = getpi(RLH, RLV);
   PI = find(PI == 1);
   PI = PI(1);
4.Extract available pupil segment through a flood-fill
  operation (Fig.3):
   P = imfill(PC, PI);
5.Fill the specular lights:
   P = rlefillsl(P);
6.Approximate the pupil by an ellipse;
OUTPUT: The ellipse approximating the pupil;
END.
```

An example of finding the pupil indicator is stated as follows:

```
function [k,PI] = getpi(RLH, RLV);
  k=16; PI = 0*RLH;
  While PI is the null matrix do:
    Compute the k-means quantization of RLV and RLH:
       RLHQ = fkmq(RLH, k);
       RLVQ = fkmq(RLV, k);
    Select the logical index of the highest cluster
    within RLHQ and RLVQ, respectively:
       LIH = ( RLHQ == max(RLHQ(:)) );
       LIV = ( RLVQ == max(RLVQ(:)) );
    Compute the binary matrix PI as logical
    conjunction of LIH and LIV:
       PI = LIH & LIV;
    k = k -1;
  EndWhile;
END.
```

We must clarify that the pupil indicator is found as a preimage corresponding to the maximum value of a fuzzy membership assignment describing the actual pupil as a subset of the pupil cluster: for each pixel within the pupil cluster, directional run-length coefficients encode the degree of membership of that pixel to the actual pupil. The argument is the fact that being (or containing) the most circular solid object within the pupil cluster, the actual pupil is the most resilient set to erosion [9] to be found in the pupil cluster. More details on this topic can be found in [12].

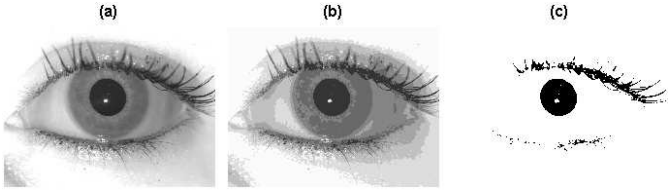

Figure 1: Original eye image (a) and its 8-means quantization (b); The pupil cluster PC (c);

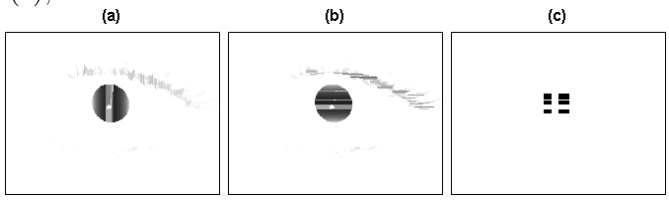

Figure 2: Vertical run-length uint8 quantization of the pupil cluster (a); Horizontal run-length quantization of the pupil cluster (b); The pupil indicator PI (c). Images are presented in binary or 8-bit complement.

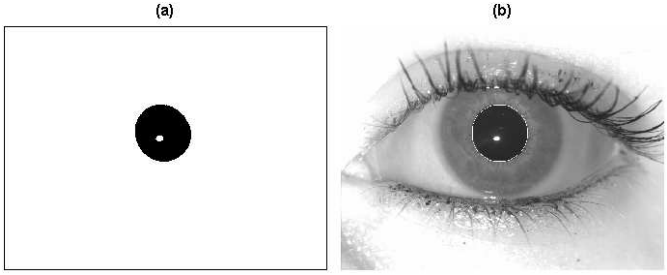

Figure 3: Extracting available pupil segment through a flood-fill operation started from any pixel within the pupil indicator (a); Approximating the pupil by an ellipse (b)

Also, the computation of the pupil indicator depends on a single parameter: a threshold for the (uint8) requantized horizontal and vertical run-length coefficients computed for the pupil cluster, threshold above which the membership of a pixel to the actual pupil is guaranteed. For these two reasons explained above, the proposed pupil finder procedure is a fuzzy approach that solves a one-dimensional optimization problem.

2.2 Limbic Boundary Approximation

The Fast Pupil Finder procedure presented above guarantees accurate pupil localization and enables us to unwrap the eye image (Fig.4.a - image from [15]) in polar coordinates (Fig.4.b) and also to practice the localization of the limbic boundary in the rectangular unwrapped eye image (Fig.4.c), obtaining an iris segment as in Fig.4.e.

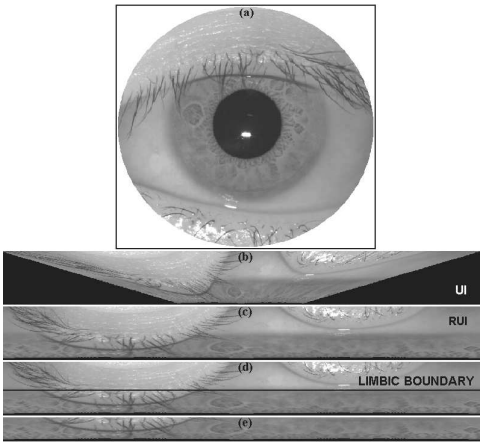

Figure 4: Iris segmentation stages

```
Circular Fuzzy Iris Segmentation Procedure (N. Popescu-Bodorin):
INPUT: the eye image IM;
1.Apply the Fast Pupil Finder procedure
   to find pupil radius and pupil center;
2.Unwrap the eye image in polar  coordinates (UI - Fig.4.b)
   through a lossless pixel-to-pixel transcoding from the circles
   within the original image to the lines within the unwrapped
   iris area UI;
3.Strech the unwrapped eye image UI
   to a rectangle (RUI - Fig.4.c);
4.Compute three column vectors: A, B, C,  where:
   A contains the means of the lines within UI matrix;
   B contains the means of the lines within RUI matrix;
   C contains the means of the lines within [A B] matrix;
5.Compute P, Q, R as being 3-means
   quantization of A, B, C, respectively (Fig.5);
6.For each line of the unwrapped eye image, count
   the votes given by P,Q and R. All the lines receiving
   at least two positive votes is assumed to belong
   to the actual iris segment;
7.Find limbic boundary and extract the iris segment
  (Fig.5, Fig.4.d, Fig.4.e);
OUTPUT: pupil center, pupil radius, index of the line
  representing limbic boundary and the final iris segment;
END.
```

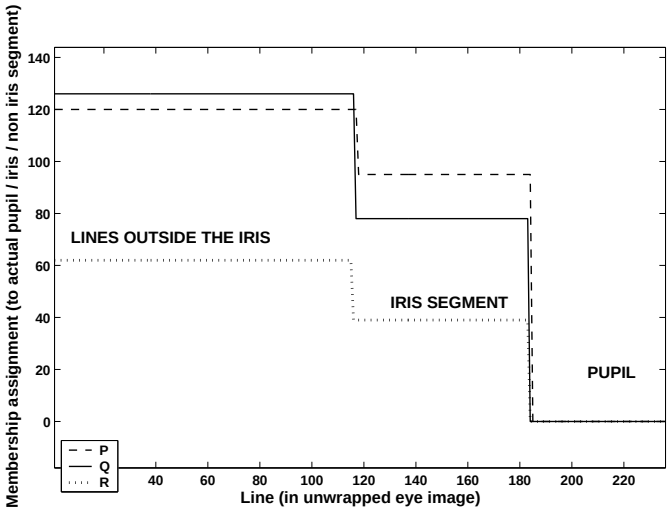

Figure 5: Iris segmentation procedure: Line assignment (step 5 of the CFIS procedure)

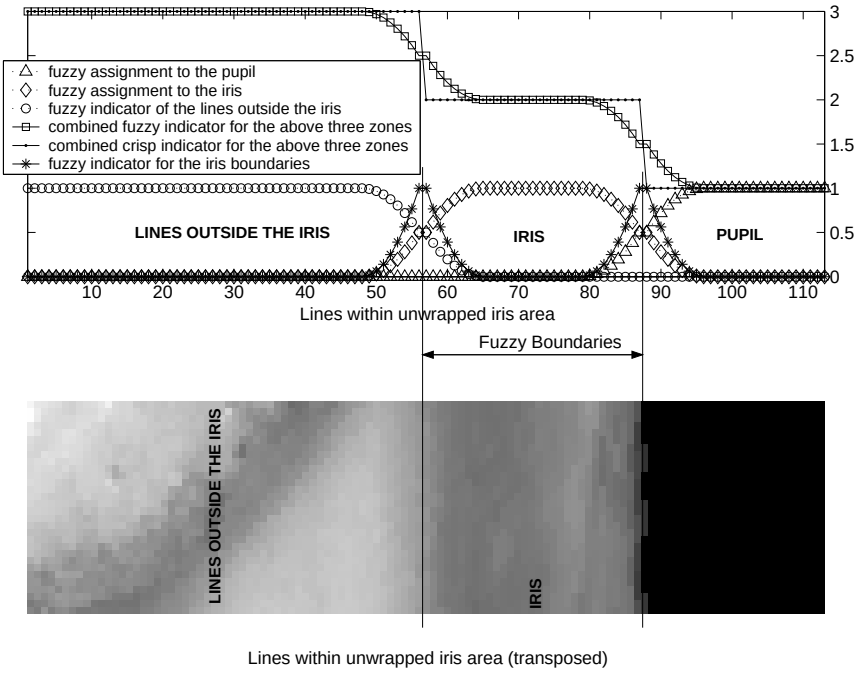

Figure 6: Fuzzy iris segment and fuzzy iris boundaries

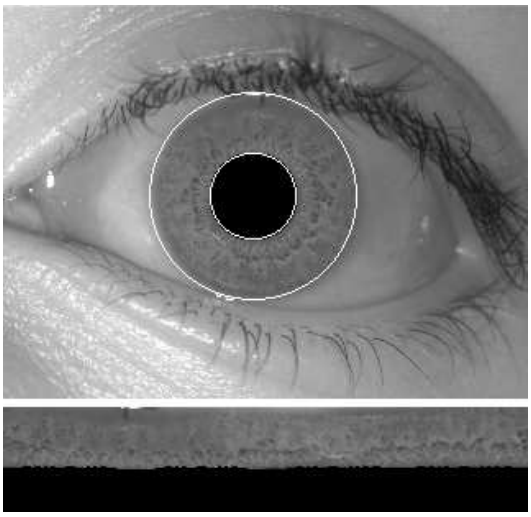

Figure 7: Circular Fuzzy Iris Segmentation Demo Program

2.3 Examples of K-Means Based Fuzzy Clusters and Fuzzy Boundaries: Fuzzy Iris Band, Fuzzy Iris Boundaries

The following two questions are among the most frequent questions asked by the readers of the previously published papers treating the above described segmentation procedure: *why should we think that CFIS is a fuzzy procedure? what is fuzzy in CFIS procedure?*

This section is meant to answer these questions.

Let us comment Fig.6 which shows what is happening with the vector B at the steps 4-5 of the CFIS procedure: hidden behind the combined crisp indicator function (crisp membership assignment) of three clusters like those marked in Fig.5 (pupil, iris and the area outside the iris) there are fuzzy membership assignment functions defined from the set of lines within rectangular unwrapped iris area (RUI) to each of the above mentioned regions and even to the iris boundaries. Hence, there is no doubt that area delimited between the fuzzy iris boundaries is the fuzzy iris band (within the rectangular unwrapped iris area RUI). Its preimage through the polar mapping is a circular fuzzy iris ring.

Three fuzzy iris bands are determined using the vectors A, B, C. The final result is computed evaluating the chances that the lines within the unwrapped iris area to belong to the actual iris segment. This is done in the step 6 of the CFIS procedure by counting the votes received for each line within the unwrapped iris area as a member of a fuzzy iris band. More details regarding the fuzzification of the iris segment and boundaries can be found in [11].

On the other hand, there is no doubt that after the pupil is found, the

limbic boundary is determined searching for a line number.

For all these reasons explained above, the proposed CFIS procedure is a fuzzy approach that solves a one-dimensional optimization problem.

A demo application illustrating CFIS (Fig.7) is available for download [14]. It can be tested using entire Bath University Iris Database [15] (the free version).

3 Gabor Analytic Iris Texture Binary Encoder

Gabor Analytic Iris Texture Binary Encoder was initially introduced in [13]. It transforms the output of CFIS procedure (unwrapped circular iris ring) into a binary iris code as follows:

Gabor Analytic Iris Texture Binary Encoder (N. Popescu-Bodorin):
INPUT: unwrapped iris segment IM (Fig.4.e), window dimenssion s, desired dimenssion $d = [d_1, d_2]$ for iris codes;

1. Compute I as being the resized version of unwrapped iris segment to desired dimenssion d;
2. For each line of I compute the complex matrix AS as being the strong analytic representation of I using window size s;
3. Compute the binary iris code IC (Fig.8)as the sign of the phase for all components within AS;
4. Compute the binary iris mask M corresponding to the various iris occlusions (specular lights, diffuse reflections, eyelashes, eyelids, etc), if any;

OUTPUT: The binary iris code IC and the binary mask M;
END.

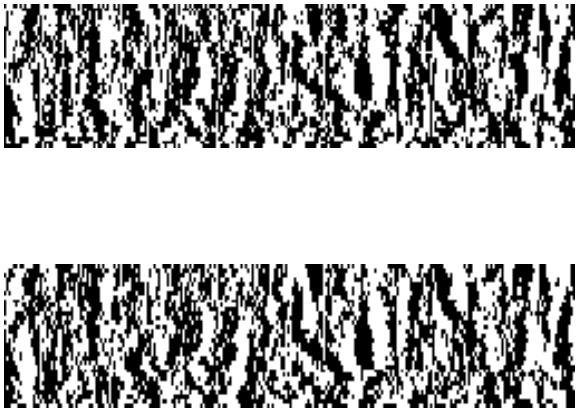

Figure 8: Two similar iris codes obtained for similar iris images ([15], 0001-L-0001.j2c, 0001-L-0003.j2c) using Gabor Analytic Iris Texture Binary Encoder

In the above encoding procedure, the term '*strong analytic representation of I*' refers to the sum of the iris segment I and its Hilbert transform calculated using blocks of dimension $1 \times s$.

Some useful details regarding the strong analytic signal, the Hilbert Transform and a synthetic example on generating iris binary code can be found in [13].

4 Experimental Results

Eleven *recognition* tests were performed using the iris images from [15] in order to prove the efficiency of the recently proposed iris recognition approach ([12], [13]) and to quantify the changes in recognition performance when using *fragile bits*. In two of these tests we have worked around two types of *fragile bits*: those caused by the phase instability ([4]) and those suspected to occur at the boundaries between regions of zeros and regions of ones ([4]). Unfortunately, the results obtained by masking these two types of *fragile bits* were weaker than the results of the tests T7, T8 and T9 (commented below) in which the *fragile bits* are assumed to be inferred from a given number of previous observation as a mask containing the pixels that are proven to be unstable by their values in 30% of the observed iris codes ([4]). For this reason, only nine of these tests are discussed here.

4.1 Terminology

In a *single-eye / single-enrollment scenario*, each identity is enrolled through a single template of one eye, while in a *single-eye/multi-enrollment scenario*, each identity is enrolled through a given number of templates sampled for the same eye.

In an *authentication scenario* the user exposes its iris to the system and claim an identity; the iris code extracted from user input is compared with the gallery templates stored under the claimed identity; the system accepts or rejects the claim depending on a similarity score computed by comparing the claming iris code to all iris codes enrolled under the claimed identity.

In a *recognition (identification) scenario* the user exposes its iris to the system and wait for the system to recognize him as an (un)enrolled identity; the system response is depending on the biggest similarity score computed by comparing the input iris code to the entire available gallery.

Hamming Similarity of two iris codes is the ratio between the number of bits that agree and the number of compared bits.

Non-match (or *imposter*, or *inter-class*) *score distribution* is the distribution of scores computed for iris codes sampled from different eyes.

Match (or *genuine*, or *intra-class*) *score distribution* is the distribution of scores computed for pairs of iris codes sampled from the same eye.

For a given threshold, the *False Accept Rate* is experimentally determined as the ratio between the number of imposter scores exceeding the threshold and the total number of imposter scores. The *False Reject Rate* (FRR) is the ratio between the number of genuine scores not exceeding the threshold and the total number of genuine scores.

The *Odds of False Accept* (OFA) is computed as cumulative of the theoretical imposter distribution above the given threshold and approximates the definite integral:

$$\int_t^1 I_{pdf}(\tau)d\tau,$$

where I_{pdf} is the theoretical probability density function of the imposter distribution and t is the threshold.

The *Odds of False Reject* (OFR) is computed as cumulative of the theoretical genuine distribution below the given threshold and approximates the definite integral:

$$\int_0^t G_{pdf}(\tau)d\tau,$$

where G_{pdf} is the theoretical probability density function of the genuine distribution and t is the threshold.

Equal Error Rate (EER) is the common value of FAR and FRR at that thresold value for which they equal each other.

4.2 A Custom Mean-Deviation Similarity Score for Multi-Enrollment Scenarios

Suppose that the value s of the standard deviation is known for the imposter score distribution. Let C be the current input iris code which must be compared to a set of templates $E = \{E_1, E_2, ..., E_n\}$ enrolled under an arbitrary identity. Consider the set of Hamming similarities between C and each of the enrolled templates: $S = \{HS(C, E_1),\ HS(C, E_2),\ ...,\ HS(C, E_n)\}$. Then the Mean-Deviation Similarity Score (N. Popescu-Bodorin) between the input template C and the arbitrary identity E is defined here as follows:

$$MDSS(C, E) = mean(S) + std(S) - s/2;$$

The above formula was heuristically determined by running a lot of tests and using neural network support to minimize the FAR and the OFA while keeping the FRR and the OFR at reasonable values (1-3%) within a given threshold range.

4.3 The Tests

The tables (1,2) present the results of nine tests undertaken to illustrate the efficiency of the recently proposed iris recognition methodology (Circular Fuzzy Iris Segmentation, Gabor Analytic Iris Texture Binary Encoder,

Mean-Deviation Similarity Score for Multi-Enrollment Iris Recognition Scenarios). All of them are recognition tests. The differences between the tests are given by changing enrollment scenarios, the lengths of the resulting iris codes, the dimension of the Hilbert filter and the type of similarity score used to compare iris codes.

The acronyms used in the Tables 1, 2 have the following meanings:
- **DF** - (Number of) Degrees-of-Freedom for a given score distribution;
- **EER** - Equal Error Rate;
- **FAR** - False Accept Rate;
- **FB** - (indicates the use of) Fragile Bits;
- **H** - Hamming Similarity Measure;
- **MDSS** - Mean-Deviation Similarity Score for *single-eye/multi-enrollment* scenarios;
- **OFA** - Odds of False Accept;
- **RSESE** - Recognition in Single-Eye/Single-Enrollment scenario.
- **RSEME** - Recognition in Single-Eye/Multiple-Enrollment scenario.
- **STD** - Standard Deviation.

In the tests (T7),(T8),(T9) the *fragile bits* are assumed to be inferred from a given number of previous observation as a mask containing the pixels that are proven to be unstable by their values in 30% of the observed iris codes, even if the causality of this instability is not evident.

For each eye, from all images available in the database, 5 images were selected as previously known observation used to compute the mask of *fragile bits*. Hence, the set of all available iris codes is spilted into two parts:
- S9, the subset containing those 125 iris codes based on which the masks of fragile bits are computed;
- S7, the complement of S9.

There are three regular single-enrollment tests (T1,T3,T5), three regular multi-enrollment tests (T2,T4,T6) and three single-enrolment tests involving *fragile bits*: (T7,T8,T9).

In the test T7, all iris codes are compared, except those 125 images from the subset S9 (5 images for each eye) while in the test T8 there is no exception. The test T9 takes into account only those 125 iris codes excepted in T7.

The purpose of these three tests (T7-9) is to show that using the masks of *fragile bits* improves recognition scores only for that set of 125 images initially used to compute the masks. For the other iris codes the results do not demonstrate a net improvement. Consequently, for the iris codes generated by GAITBE, each mask of this type depends mainly on the given set of observations and it is not a true feature of the iris. Consequently, the set set of genuine scores is splited into two distributions having two completely different statistics (see Fig.10) and the apparent improvements of the recognition performance measured through decidability index and through Fisher's ratio are, in fact, irrelevant.

Table 1: Statistics of experimental data

TEST ID	(T1)	(T2)	(T3)	(T4)	(T5)	(T6)	(T7)	(T8)	(T9)
Code length:	192	192	768	768	512	512	512	512	512
Window size:	1x8	1x8	1x16	1x16	1x8	1x8	1x8	1x8	1x8
Similarity	H	MDSS	H	MDSS	H	MDSS	H	H	H
Comparison type	1-1	1-5	1-1	1-5	1-1	1-5	1-1FB	1-1FB	1-1FB
Test/System type	RSESE	RSEME	RSESE	RSEME	RSESE	RSEME	RSESE	RSESE	RSESE
INTER-CLASS									
Mean	0.5038	0.5049	0.5038	0.5031	0.5030	0.5041	0.5059	0.5062	0.5072
Median	0.5039	0.5049	0.5037	0.5030	0.5030	0.5041	0.5058	0.5061	0.5067
STD	0.0193	0.0169	0.0166	0.0152	0.0156	0.0135	0.0256	0.0264	0.0284
DF	669	875	909	1089	1030	1374	380	360	309
Skewness	-0.0079	-0.0066	0.0024	0.0266	0.0115	0.0470	0.0213	0.0372	0.0823
Kurtosis	0.0366	0.0392	0.0488	0.0464	0.1454	0.1878	0.0648	0.0624	-0.0040
Minim	0.4167	0.4367	0.4351	0.4452	0.4273	0.4406	0.3896	0.3837	0.3946
Maxim	0.5918	0.5716	0.5754	0.5639	0.5799	0.5632	0.6279	0.6279	0.6113
Width	0.1751	0.1349	0.1403	0.1187	0.1526	0.1226	0.2383	0.2442	0.2167
INTRA-CLASS									
Mean	0.6718	0.7039	0.6678	0.6993	0.6684	0.6988	0.7207	0.7363	0.7993
Median	0.6706	0.7019	0.6659	0.6962	0.6666	0.6953	0.7209	0.7367	0.8005
STD	0.0550	0.0464	0.0533	0.0467	0.0502	0.0440	0.0497	0.0526	0.0370
DF	73	97	78	96	88	109	81	70	117
Skewness	0.3528	0.2200	0.4547	0.2851	0.4253	0.1883	-0.0051	-0.0563	-0.2802
Kurtosis	1.0995	0.1246	1.3840	0.1627	1.5520	0.1808	1.1405	0.6118	0.3234
Minim	0.4909	0.5454	0.4884	0.5489	0.4952	0.5424	0.5152	0.5152	0.6547
Maxim	1	0.8450	1	0.8353	1	0.8303	1	1	0.9072
Width	0.5091	0.2996	0.5116	0.2864	0.5048	0.2880	0.4848	0.4848	0.2525
Overlap	0.1009	0.0262	0.0869	0.0150	0.0847	0.0208	0.1127	0.1127	0

Table 2: Statistics of Experimental Data (continued)

TEST ID	(T1)	(T2)	(T3)	(T4)	(T5)	(T6)	(T7)	(T8)	(T9)
Overlap	0.1009	0.0262	0.0869	0.0150	0.0847	0.0208	0.1127	0.1127	0
Decidability	4.0794	5.6943	4.1555	5.6495	4.4492	5.9865	5.4272	5.5336	8.8488
Fisher ratio	8.3208	16.212	8.6340	15.958	9.8975	17.919	14.727	15.310	39.150
EER	0.0126	1.3E-3	9.3E-3	1.3E-3	7.5E- 3	1.3E-3	4.4E-3	3.9E-3	0
At a FAR of: 0.001									
FRR	0.0222	0.0013	0.0159	0.0013	0.0115	0.0013	0.0087	0.0064	0
Threshold	0.5635	0.5570	0.5555	0.5503	0.5531	0.5488	.58718	.58988	.59668
At a FRR of 0.01:									
FAR	0.0243	0	0.0072	0	0.0020	0	6.29E-4	1.43E-4	0
OFA	0.0232	2.1E-09	0.0068	1.5E-10	0.0015	3.2E-13	4.54E-4	1.16E-4	2.3E-12
OFR	0.0092	0.0160	0.0105	0.0155	0.0088	0.0131	0.0046	0.0057	0.0050
Threshold	.54231	.60429	.54475	.59847	.54924	.60112	.59097	.60319	.70399
At a threshold of:	**0.59**	**0.59**	**0.59**	**0.59**	**0.59**	**0.59**	**0.63**	**0.63**	**0.63**
FRR	0.0564	0.0027	0.0587	0.0054	0.0510	0.0081	0.0380	0.0251	0
OFR	0.0682	0.0071	0.0721	0.0097	0.0592	0.0067	0.0342	0.0216	2.4E-6
FAR	2.1E-6	0	0	0	0	0	0	0	0
OFA	4.1E-6	2.4E-7	1.0E-7	4.9E-9	1.2E-8	9.7E-11	6.5E-7	1.3E-6	7.9E-6
At a threshold of:	**0.6**	**0.6**	**0.6**	**0.6**	**0.6**	**0.6**	**0.64**	**0.64**	**0.64**
FRR	0.0806	0.0081	0.0853	0.0107	0.0717	0.0094	0.0504	0.0335	0
OFR	0.0955	0.0126	0.1016	0.0168	0.0865	0.0123	0.0524	0.0335	8.4E-6
FAR	0	0	0	0	0	0	0	0	0
OFA	3.2E-7	9.3E-9	3.3E-9	8E-11	2.4E-10	5.9E-13	8.5E-8	1.9E-7	1.5E-6

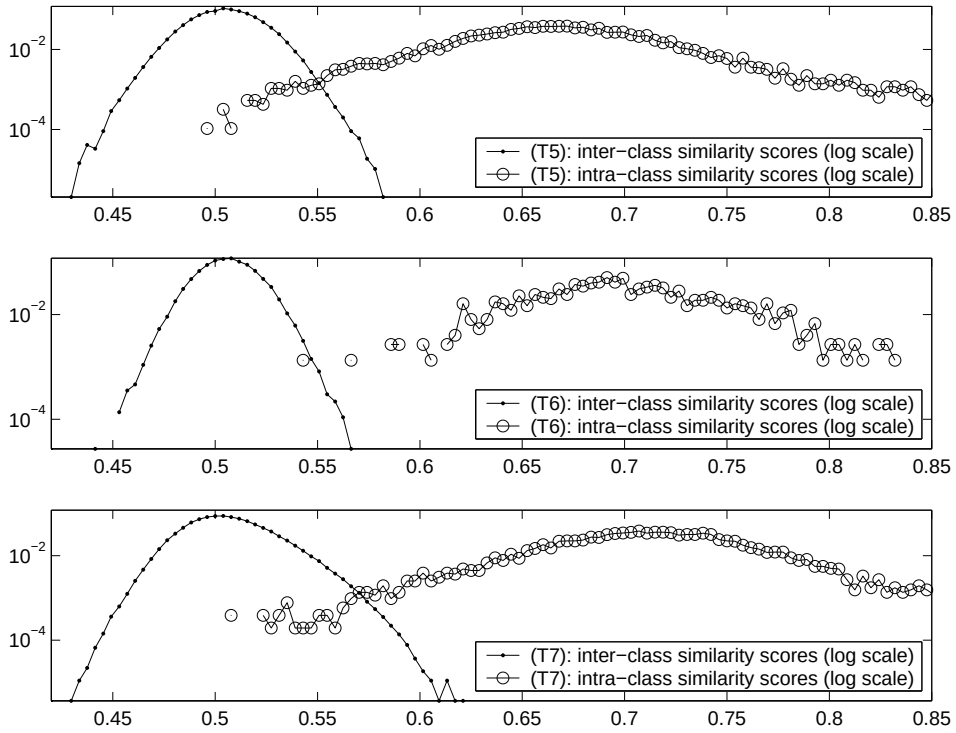

Figure 9: Inter/intra-class distributions for the tests T5, T6 and T7 (from top to buttom)

Using the same 125 images from the subset S9 as enrollment samples and using the Mean-Deviation Similarity Score, the tests T2, T4 and T6 give us a measure about what an improvement really is.

Also, by comparing the tests (T1, T2), (T3, T4) and (T5, T6), it can be seen that increasing the quantity of *a priori knowledge* (T2, T4, T6) decreases the imposter-genuine decision uncertainty in terms of:

- narrowing the ranges of both distributions and their overlapping interval;
- decreasing the standard deviation in each class of scores;
- better encoding of the statistical independence between iris codes representing different eyes;
- decreasing the Odds of False Accept and the actual False Accept Rates computed for threshold values within the neighborhood of the observed maximum imposter score;
- decreasing the tail thickness for both distributions of scores;
- decreasing the Odds of False Accept and the actual False Accept Rates at a given False Reject Rate of 1%;

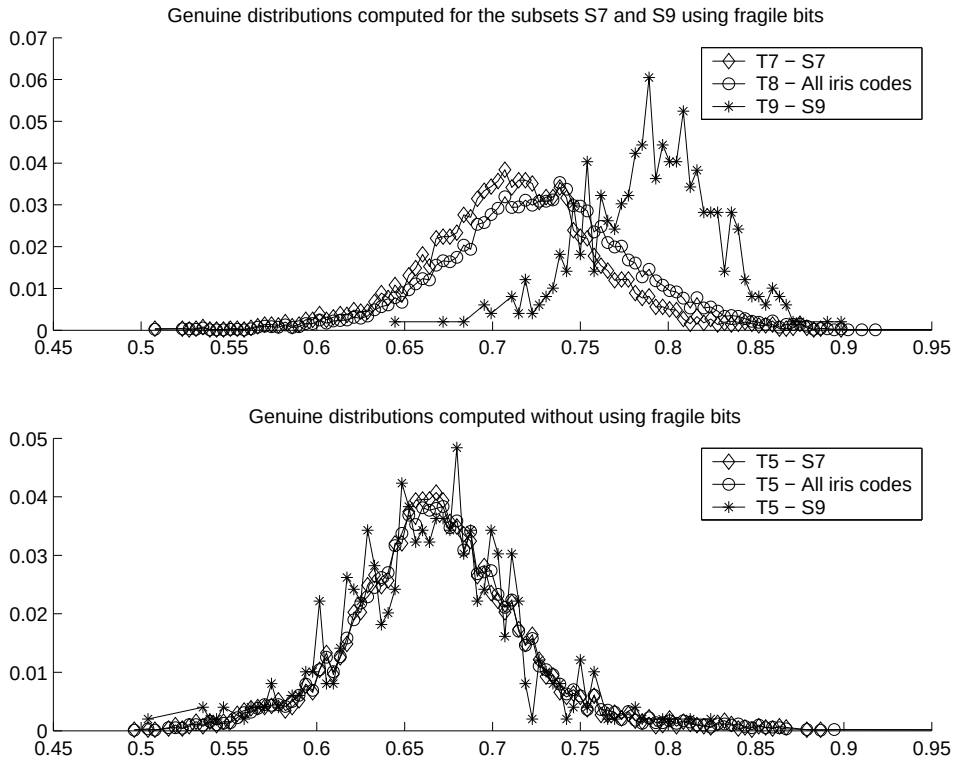

Figure 10: Analyzing the effects of using fragile bits

- decreasing the Odds of False Reject and the actual False Reject Rates at a given False Accept Rate of 0.1%.

Also, the way in which *a priori knowledge* is added to a biometric system proved to be very important:

- when defining identities through a collection of enrolled templates (T2, T4, T6) each identity includes a little variability and the intra-class distribution becomes narrower and so does the inter-class distribution (the fact that iris codes of different irides match each other by chance becomes more obvious in the experimental data);
- by contrast, inferring the existence of a mask of *fragile bits* defined as in T7, T8 and T9 produces a weaker (and contestable) improvement in recognition performance. By comparing the tests (T5,T6) and (T5,T7) it can be seen that, in the test T7, the bigger distance between the means of the genuine and imposter score distributions is compensated by an increase in their standard deviations;
- the tests T5 and T7 show that the mean of the intra-class distribution increases with 8% and the width of intra-class distribution decreases with 4%, but unfortunately, the width of inter-class distribution increases with 26%;

- a totally different situation is revealed by comparing the tests T5 and T6; the mean of the intra-class distribution increases with 4.5% and the widths of both inter/intra-class distributions decrease with 19.6% and 43%, respectively.

All remarks from above are illustrated in Fig.9 and Fig.10. For comparison, the Tables 1, 2 and the following resources will certainly be useful:

- Fig.3 in [10], where similar results (FRR values at a FAR of 0.001) are presented for three state-of-the-art iris recognition algorithms evaluated in ICE 2006 [8]: CAM-2 (Cambridge), IrTch-2 (IriTech), SI-2 (Sagem-Iridian);
- Table 1 in [17], Fig.5 in [7], Fig.5 in [6], Fig.9 in [5].

5 Conclusion and Future Works

This paper proved that using the proposed methodology and implementing iris recognition in *multiple-enrollment scenario* lead to very good performances.

Only minor (and contestable) improvements had been obtained using the concept of *fragile bits*. For the iris codes generated with Gabor Analytic Iris Texture Binary Encoder, the mask of *fragile bits* proved to be a strong feature of a given set of observations (mainly influenced by the acquisition process), but a weak feature of the observed iris.

Future works will explore the possibilities of reducing the number of comparisons which are needed in order to obtain a recognition decision in a multi-enrollment scenario.

Acknowledgment

The author wishes to thank Professor Luminita State (University of Pitesti, RO) for the comments, criticism, and constant moral and scientific support during the last two years. The author would also like to thank Professor Donald Monro (University of Bath, UK) for granting the access to the Bath University Iris Database.

References

[1] R.M. Bolle, S. Pankanti, J.H. Connell, and N. Ratha, *Iris Individuality: A Partial Iris Model*, Proceedings of the 17^{th} Intl Confference on Pattern Recognition, pp. II: 927-930, 2004.

[2] J.G. Daugman, *High Confidence Visual Recognition of Persons by a Test of Statistical Independence*, IEEE TPAMI, Vol. 15, No. 11, November 1993.

[3] J.G. Daugman, *New Methods in Iris Recognition*, IEEE TSMC, vol. 37, no. 5, october 2007.

[4] K.P. Hollingsworth, K.W. Bowyer, P.J. Flynn, *The Best Bits in an Iris Code*, IEEE TPAMI, vol.31, no. 6, June 2009.

[5] X. Liu, K. W. Bowyer, P. J. Flynn, *Experiments with an Improved Iris Segmentation Algorithm*, Proceedings of the Fourth IEEE Workshop on Automatic Identification Advanced Technologies, pp. 118-123, 2005.

[6] L. Ma, T. Tan, Y. Wang, D. Zhang, *Efficient Iris Recognition by Characterizing Key Local Variations*, IEEE Trans. on Image Processing, vol. 13, no. 6, June 2004.

[7] D. M. Monro, S. Rakshit, *Rotation Compensated Human Iris Matching*, IEEE Workshop on Signal Processing Applications for Public Security and Forensics, 2007.

[8] National Institute of Standards and Technology, *Iris Challenge Evaluation*, http://iris.nist.gov/ice/

[9] W. Pegden, *Sets resilient to erosion*, web reference at Department of Mathematics, Rutgers University, June 2008, http://people.cs.uchicago.edu/~wes/erosion.pdf

[10] P. J. Phillips, W. T. Scruggs, A. J. OToole, P. J. Flynn, K. W. Bowyer, C. L. Schott, M. Sharpe, *Face Recognition Vendor Test 2006 and Iris Challenge Evaluation 2006 Large-Scale Results*, National Institute of Standards and Technology, March 2007.
http://iris.nist.gov/ice/FRVT2006andICE2006LargeScaleReport.pdf

[11] N. Popescu-Bodorin, *A Fuzzy View on k-Means Based Signal Quantization with Application in Iris Segmentation*, 17th Telecommunications Forum - TELFOR 2009, Belgrade, November 2009,
http://fmi.spiruharet.ro/bodorin/articles/telfor09.pdf

[12] N. Popescu-Bodorin, *Circular Fuzzy Iris Segmentation*, Proceedings of the 4^{th} Annual South East European Doctoral Student Conference, vol. 1, pp. 471-479, South-East European Research Centre, Thessaloniki, July 2009.

[13] N. Popescu-Bodorin, *Gabor Analytic Iris Texture Binary Encoder*, Proceedings of the 4^{th} Annual South East European Doctoral Student Conference, vol. 1, pp. 505-513, South-East European Research Centre, Thessaloniki, July 2009.

[14] N. Popescu-Bodorin, *Circular Fast Fuzzy Iris Segmentation and Fast k-Means Quantization Demo Programs*, June 2009,
http://fmi.spiruharet.ro/bodorin/arch/cffis.zip, fkmq.zip.

[15] University of Bath Iris Database,
http://www.bath.ac.uk/elec-eng/research/sipg/irisweb/

[16] R.P. Wildes, *Iris Recognition - An Emerging Biometric Technology*, Proceedings of the IEEE, Vol. 85, No. 9, September 1997.

[17] S. Ziauddin, M. N. Dailey, *Iris Recognition Performance Enhacement using Weighted Majority Voting*, ICIP, 2008,
http://www.cs.ait.ac.th/ mdailey/papers/Ziauddin-WeightedMajority.pdf